Pharmaceutical Research, Vol. 25, No. 5, May 2008 (© 2007)
DOI: 10.1007/s11095-007-9526-7

Research Paper

Design of Biodegradable Hydrogel for the Local and Sustained Delivery of Angiogenic Plasmid DNA

Hyun Joon Kong,[1,2] Eun Seok Kim,[1,3] Yen-Chen Huang,[4] and David J. Mooney[1,5]

Received October 23, 2007; accepted December 10, 2007; published online January 9, 2008

Purpose. To attain the effective local and sustained delivery of plasmid DNA (pDNA) encoding for a growth factor.
Methods. We hypothesized that controlling the degradation rate of biomaterials encapsulating pDNA via concurrent physical dissociation of the cross-linked structure and hydrolytic chain breakage of polymers would allow one to significantly broaden the range of pDNA release rate. This hypothesis was examined using ionically cross-linked polysaccharide hydrogels which were previously designed to rapidly degrade via engineering of ionic cross-linking junction and partial oxidation of polysaccharide chains.
Results. The hydrogel degradation rates were varied over the broad range, and pDNA release correlated with the gel degradation rate. Degradable hydrogels were used for the local and sustained delivery of a pDNA encoding for vascular endothelial growth factor (VEGF) in the ischemic hindlimbs of mice, and local pDNA release significantly improved the recovery of blood perfusion as compared with a bolus injection of VEGFencoding pDNA.
Conclusions. This strategy to control the hydrogel degradation rate may be useful in regulating the delivery of a broad array of macromolecular drugs, and subsequently improve their therapeutic efficacy.

KEY WORDS: blood perfusion; degradation; gene expression; therapeutic angiogenesis.

INTRODUCTION

Therapeutic angiogenesis aims to engineer blood vessel regeneration, and has shown promise to improve the repair and recreation of the circulatory system after induction of ischemia, tissue transplantation, and biomedical device implantation (1–5). This approach has been implemented with a variety of bioactive macromolecular drugs [e.g., recombinant vascular endothelial growth factor (VEGF) (2, 6, 7), genes encoding for VEGF (3, 8–11)] that stimulate proliferation and differentiation of host and transplanted endothelial cells and their precursors.

Non-viral gene therapy using pDNA encoding for angiogenic growth factors (e.g., VEGF) is attractive due to several advantages over growth factors (i.e., extended bioactivity) and viral gene therapy (i.e., lack of immunogenicity) (8–11). These molecules are commonly used in the form of a complex with cationic lipids or polycations, in order to improve the efficiency of gene transfer and subsequent VEGF expression level (12–17). These VEGF-encoding pDNA complexes are commonly delivered to target tissue via intravascular or intramuscular injection (6, 8, 18), but local and sustained delivery of pDNA may be advantageous to increase the success of gene-based therapeutic angiogenesis (19–23).

Significant efforts to control gene delivery have been made by incorporating pDNAs into biodegradable materials processed in the physical forms of microparticles, micelles, hydrogels, and porous matrices. (6, 22–25). Hydrogels are increasingly used as gene delivery vehicles, because they are injectable and structurally similar to extracellular matrices (26–29). The pDNA release rate from the gel matrices is commonly regulated with the degradation rate of the gel (26–29), because the material degradation caused by various intrinsic and extrinsic factors increases the diffusion rate of pDNAs. However, side-products formed via the biomaterial degradation may denature biomacromolecules, and this may have limited the effective range of pDNA release. Recently, we have shown that biomaterial degradation can be regulated via simple physical dissociation of polymer chains in ionically cross-linked hydrogels, in combination with low levels of hydrolytic chain breakage (30, 31). Specifically, calcium cross-linked alginate hydrogels consisting of partially oxidized alginates having different molecular weights (MW) will be used to form gels (30, 31). Exclusive cross-linking between blocks of guluronic acid (GA) residues, namely GA blocks, occurs in this system and thus the molecular weight of the GA block is a significant factor regulating the physical properties of the hydrogels. This degradation mechanism may circumvent concerns regarding the denaturation of pDNA caused by degradation products.

[1] Division of Engineering and Applied Sciences, Harvard University, Cambridge, Massachusetts 02138, USA.
[2] Department of Chemical and Biomolecular Engineering, Institute for Genomic Biology, University of Illinois at Urbana-Champaign, Urbana, Illinois 48109, USA.
[3] School of Medicine, Chungnam National University, Daejeon, South Korea.
[4] Department of Biomedical Engineering, University of Michigan, Ann Arbor, Michigan 48109, USA.
[5] To whom correspondence should be addressed. (e-mail: mooneyd@seas.harvard.edu)

We hypothesized in this study that the alginate gel degradation could be manipulated to regulate the rate of pDNA release, while leading to little or no loss of pDNA activity. Two types of alginate with varying molecular weight of the GA blocks were mixed to create a size mismatch between polymer segments responsible for ionic cross-linking. The pDNA release rate and subsequent cellular exogenous expression of the pDNA released from various gels was monitored. Finally, rapidly degrading hydrogels were used to deliver pDNA encoding for VEGF to ischemic hindlimbs of mice in order to test whether this material system could improve the efficacy of gene-based therapeutic angiogenesis.

EXPERIMENTAL AND METHODS

Modification and Characterization of Alginate Molecules

High molecular weight (MW) sodium alginates with high guluronic acid (GA) residue content (MVG, FMC Technologies) [Fig. 1a] and high MW sodium alginates with low GA residue content and high mannuronic acid (MA) residue content [Fig. 1b] (MVM, FMC Technologies) were used in this study. MW of MVG was decreased by irradiating solid granules at a dose of 5 mrad with a cobalt-60 source. However, the MWs of GA blocks (cross-linking junction) in both MVG and low MW MVG are much higher than the MW of GA blocks in MVM, as we previously demonstrated (30). MVG, MVM, and irradiated low MW MVG were oxidized with sodium periodate ($NaIO_4$, Aldrich Chemicals) to induce the acetal linkage cleavable by hydrolysis [Fig. 1c] (31). The fraction of oxidized sugar residues within single alginate chains was kept constant at 0.01. After reaction for 24 h, the unreacted $NaIO_4$ was neutralized with ethylene glycol (Aldrich Chemicals). After filtering, the alginate solutions were dialyzed with membranes to remove molecules smaller than 1,000 g/mol. The oxidized alginates were reconstituted with Dulbecco's modified Eagle's medium (DMEM, Invitrogen) to 2% (*w*/*w*) solutions, following filtration for sterilization and lyophilization.

The MW of alginates was determined with a size-exclusion chromatographic system (Viscotek) equipped with a laser refractometer (LR 40), a differential viscometer (T60), and a right angle laser light scattering detector (RALLS) (31). 0.1 M $NaNO_3$ buffer solution (pH 6.3) was used as a mobile phase, and alginates were dissolved in the mobile phase.

Preparation and Characterization of Hydrogels

Calcium cross-linked alginate hydrogels were prepared by mixing 2% (*w*/*w*) alginate solutions with calcium sulfate ($CaSO_4$, Sigma) slurries. Three different hydrogels, termed as MVG gel, oxidized binary MVG gel, and oxidized binary MVM gel, were prepared with four different alginate molecules [Table I]; high MW alginate with high GA residue content (High MW MVG,), partially oxidized high MW alginate with high GA residue content (Oxidized High MW MVG), partially oxidized low MW alginate with high GA residue content (Oxidized Low MW MVG), and partially oxidized high MW alginate with low GA residue content (Oxidized High MW MVM). The unary MVG gel was prepared solely with high MW MVG [Fig. 1d]. Oxidized binary MVG gel was prepared by cross-linking a mixture of oxidized high MW MVG and oxidized low MW MVG [Fig. 1e]. The oxidized binary MVM gel was prepared by cross-linking a mixture of oxidized high MW MVM and oxidized low MW MVG [Fig. 1f]. In binary gels, the volume ratio between the two alginates types was kept constant at 1:1. The molar ratio between calcium and alginate sugar residues was kept constant at 1.0:0.3 in all gels. The mixtures were immediately cast between glass plates separated with 2 mm spacers, and after 2 h the gels were cut into disks (24 mm diameter). The gels were stored at 37°C in DMEM for a day before testing.

Fig. 1. Chemical structure of the uronic acid residues in alginate molecules and schematic description of the hydrogel microstructures. Alginate molecules consist of blocks of guluronic acid (*GA*) residues (**a**) and blocks of mannuronic acid (*MA*) residues (**b**). Oxidation of alginate molecules opens the sugar ring of MA residues to form acetal linkages (**c**). Hydrogels were formed from regular alginates and partially oxidized alginates with different overall molecular weights and different molecular weights of the blocks of guluronic acid (*GA*) residues. Unary MVG gels consisted of high MW MVG, and are hypothesized to undergo slow dissociation between GA residues (**d**). Oxidized binary MVG gels consisted of oxidized high MW MVG and oxidized low MW MVG, and are hypothesized to degrade at intermediate rates via hydrolytic cleavage of acetal linkages in oxidized uronic residues (**e**). Oxidized binary MVM gels consisted of oxidized high MW MVM and low MW MVG, and are hypothesized to degrade rapidly, due to hydrolytic cleavage of acetal linkages in oxidized uronic acid residues and accelerated dissociation between GA residues. (**f**). *Closed circle* represents the domains that may degrade via hydrolysis and *open circle* represents the cross-linked domains that may be rapidly dissociated via ion-exchange.

The elastic modulus (E) of the gels was measured by compressing at a constant deformation rate of 1 mm/min with a mechanical tester (MTS Bionix 100, MTS systems) at 25°C. From the strain limited to the first 10%, and the resulting stresses (σ), the compressive elastic moduli of the hydrogels were calculated. Assuming that the alginate hydrogels fit an affine network model, the shear modulus (S) was obtained from the slope σ *vs* $-(\lambda-\lambda^{-2})$ plot, where λ is the ratio of the deformed length to the undeformed length of the hydrogel.

The swelling ratios of the gels at equilibrium were also determined by measuring the weights of swollen gels following incubation at 37°C for 24 h, and the weight of dried alginate in each gel. The degree of swelling (Q) was defined as the reciprocal of the volume fraction of a polymer in a hydrogel (v_2)

$$Q = \frac{1}{v_2} = \left[\frac{1}{\rho_p}\left(\frac{Q_m}{\rho_s} + \frac{1}{\rho_p}\right)^{-1}\right]^{-1} \quad (1)$$

where ρ_p is the polymer density (0.8755 g cm^{-3}), ρ_s is the density of water, and Q_m is the swelling ratio, defined as the mass ratio of absorbed water to the dried gel. From S and Q, the effective number of cross-links (N) was determined based on the rubber elasticity theory (32)

$$N = \frac{SQ^{-1/3}}{RT} \quad (2)$$

where R is the gas constant (8.314 J mol^{-1} K^{-1}), and T is the temperature at which the modulus was measured.

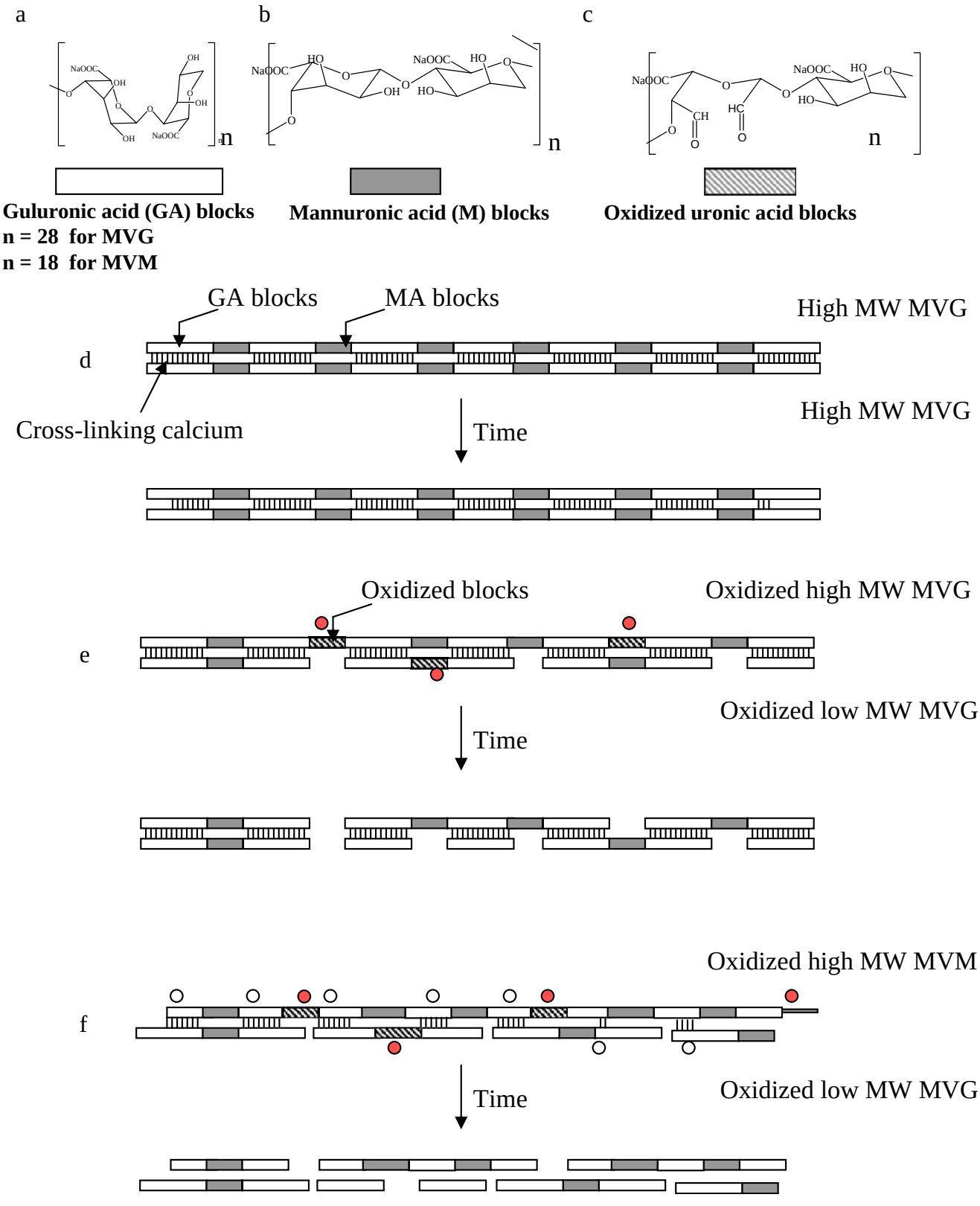

The degradation rate of hydrogel was evaluated from the decrease of N over time. The E and Q of the gels were monitored on a weekly basis. The DMEM was also exchanged on a weekly basis.

Release Study of pDNA

The gWiz vector containing the gene encoding for luciferase (Aldevron) was combined with linear poly(ethyl-

eneimine) [PEI, MW ~ 22,000 g/mol] (Fermentas) to form a polyelectrolyte complex as previously described (33). The ratio of the number of amine groups in PEI and the number of phosphate groups (N/P ratio) in pDNA was kept constant at 7. In certain experiments, naked pDNA and pDNA-PEI complexes prepared at the N/P ratio of 20 were used. The pDNA-PEI complexes were encapsulated in hydrogels at a concentration of 100 μg pDNA/ml, and hydrogels were incubated at 37°C in DMEM. The concentration of pDNA released into the medium was measured using Quant-iT™ PicoGreen® dsDNA Assay Kit (Invitrogen).

In Vitro Gene Expression Assay

The gWiz vector containing the gene encoding green fluorescent protein (GFP) [Aldevron] was combined with linear PEI and the resulting pDNA-PEI complexes were encapsulated in the MVG gel and oxidized binary MVM gel at a concentration of 100 μg pDNA/ml. The hydrogels were embedded in a bovine type I collagen gel matrix, within which murine MC3T3-E1 pre-osteoblasts were embedded. The collagen gel matrix was formed by adjusting pH of collagen solution supplemented with FBS and DMEM to pH 7.3 followed by incubation at 37°C. Pre-osteoblasts, a generous gift from Dr. Renny T. Franceschi at the University of Michigan, were mixed with collagen solution at neutral pH prior to gel formation. The cell density in the collagen matrix was kept constant at 100,000 cells/ml. The expression level of GFP in cells was evaluated by quantifying green fluorescence in transfected cells over 2 weeks in order to examine whether the GFP expression was maintained over a time frame consistent with the biological processes of interest. Fluorescent images were captured using a conventional fluorescence microscope (Olympus).

Alternatively, the gWiz vector containing the gene encoding luciferase [Aldevron] was combined with linear PEI, and the resulting pDNA-PEI complexes were encapsulated in the MVG gel and oxidized binary MVM gel at a concentration of 100 μg pDNA/ml. Hydrogels were embedded in a bovine type I collagen gel matrix with C2C12 skeletal myoblasts (ATCC) as described above. For the measurement of the expression level of luciferase, the cells were collected by digesting the collagen gel matrix with collagenase (Invotrogen), and they were lysed with cell lysis buffer (Promega). The cell lysates collected following the ultracentrifugation were mixed with Dual-Glo™ luciferase assay reagents (Promega). The luminescence from the mixture was recorded with a plate reader (BioTek).

Revascularization Study

The femoral artery of NOD mice (Jackson Laboratory) was ligated and the exposed artery ends were tied off with nylon sutures to create hindlimb ischemia as previously described (34). The gWiz vector containing the gene encoding for $VEGF_{165}$, a generous gift from Dr. Douglas W. Losordo at Tufts University, was combined with linear PEI to form the pDNA-PEI complex (19). A solution containing the complex in PBS was injected into a pocket between muscle and connective tissue adjacent to the ligation site, at a dose of 25 μg pDNA per animal. Alternatively, the complexed pDNA was encapsulated into the oxidized binary MVM gel and injected into the connective tissue. In addition, the ligation site was exposed to a PBS solution or oxidized binary MVM gels not containing pDNA as controls. The treatment of experimental animals was in accordance with NIH animal handling procedures.

The blood flow ratio between the ischemic limb and normal limb of the same animal was measured with a laser Doppler perfusion imaging system (Perimed AB) on a weekly basis in order to evaluate the recovery of blood perfusion. The entire hindlimbs of anesthetized mice ($n=4$) were scanned. The recovery was quantified by the ratio of ischemic to nonischemic limb blood flow. After 40 days, the mice were sacrificed, and tissues surrounding the ligated artery were collected. The tissues were fixed in zinc–formalin solution at 4°C overnight and dehydrated through graded ethanol, embedded in paraffin and cut into 4 mm sections.

Blood vessels in tissue sections were identified with antibodies raised against mouse CD 31 (Pharmingen) using a blocking solution, universal secondary antibody, straptevidin/horseradish peroxidase (HRP) (Biocare Medical), and diaminobenzidine (Zymed) as previously described (6). The number of blood vessels was also counted to calculate the density of blood vessels in the connective tissue and muscle.

RESULTS

Chemical Modification of Alginate

The molecular weight (MW) of alginate was adjusted with γ-irradiation, and hydrolytically cleavable segments were introduced into alginate chains via oxidation. Specifically, low MW MVG (MW ~ 50,000 g/mol) was obtained by irradiating high MW MVG (MW ~ 270,000 g/mol). Oxidized high MW MVG and low MW MVG were obtained by oxidizing the MVG and low MW MVG polymers. The fraction of oxidized uronic acid residues in a single polymer chain was kept constant at 0.01. Oxidation led to a decrease in the MW of alginates (i.e., for high MW MVG: from 270,000 to 180,000 g/mol, for high MW MVM: from 280,000 to 160,000 g/mol, and for low MW alginate: 60,000 to 40,000 g/mol). In contrast, irradiation at 5 mrad and oxidation of 1 mol% resulted in a minimal change in the molecular weight of the GA blocks (MW_{GA}) in the polymer chains, as reported previously (31). Therefore, MW_{GA} in high MW MVG, oxidized high MW MVG, and oxidized low MW MVG were 5,500 g/mol (i.e., number of guluronic acid residue in a GA block is 28), while MW_{GA} in oxidized high MW MVM was 3,600 g/mol (i.e.; number of guluronic acid residue in a GA block is 18) (31).

Degradation of Hydrogels

Three different gels were prepared with the four different alginate molecules, including unary MVG gels solely consisting of high MW MVG [Fig. 1d], oxidized binary MVG gels consisting of oxidized high MW MVG and oxidized low MW MVG [Fig. 1e], and oxidized binary MVM gels consisting of oxidized high MW MVM and oxidized low MW MVG [Fig. 1f]. The oxidized binary MVG and oxidized binary MVM gels contained oxidized sugar residues that may be cleaved by hydrolysis of acetal linkages, and a mismatch in

Table I. Formulation of Hydrogels and Physical Properties of the Fresh Hydrogels

Hydrogel	$\Phi_{\text{high MW MVG}}$	$\Phi_{\text{oxidized high MW MVG}}$	$\Phi_{\text{oxidized low MW MVG}}$	$\Phi_{\text{oxidized high MW MVM}}$	E_0 (kPa)	Q_0	N_0 ($\times 10^{-7}$ mol/cm^3)
Unary MVG	0.02				35±3	27±1	47±5
Oxidized binary MVG		0.01	0.01		23±4	30±2	30±5
Oxidized binary MVM			0.01	0.01	8±1	38±2	10±0.3

Values represent mean and standard deviation.
Φ volume fraction of polymer in the hydrogel, E_0 elastic modulus of the fresh gel, Q_0 swelling ratio of the fresh gel, N_0 initial cross-link number in the gels.

the cross-linking junction (GA blocks with different molecular weights) was present in the oxidized binary MVM gels (30, 31). The elastic moduli (E_0) and swelling ratios (Q_0) of fresh hydrogels were altered with the hydrogel formulation [Table I]. Specifically, E_0 and $1/Q_0$ decreased in the order of unary MVG gel, oxidized binary MVG gel, and oxidized binary MVM gel, and the number of cross-links (N) calculated using Eq. 2 was similarly decreased in these gels.

The degradation rates of the hydrogels were quantified by the decrease of N over time. Interestingly, N of the oxidized binary gels decreased more rapidly than N of unary MVG gels, which are known to slowly degrade via ion exchange that leads to separation of cross-linked GA blocks [Fig. 2a]. In addition, the oxidized binary MVM gels had the faster decreases of N, and were largely dissolved within 20 days. The decrease of N over time (t) followed first-order degradation kinetics [Eq. 3].

$$\frac{N_t}{N_0} = \exp(-k_1 t) \tag{3}$$

The degradation rate constant (k_1) was significantly increased in more rapidly degrading gels [Table II].

Control of pDNA Release from Hydrogels

The pDNA release rates from the various hydrogels were next examined. The unary MVG gel did not exhibit significant release of pDNA over 20 days, while the oxidized binary MVM gel released 90% of the originally encapsulated pDNA within 10 days [Fig. 3a]. The oxidized binary MVG gel, which degraded at an intermediate rate also led to an intermediate pDNA release rate. No significant dependency of the release rate on the N/P ratio of pDNA-PEI complexes was found, although naked pDNA was released from the oxidized binary MVM hydrogel more slowly than pDNA-PEI complexes [results not shown]. The pDNAs in the oxidized binary MVG and MVM hydrogels remained structurally stable, as confirmed with gel electrophoresis of pDNA (data not shown). The pDNA release rate (k_2) was quantified by fitting the decrease of the pDNA concentration in the hydrogel (C_{DNA}) over time to first-order drug release kinetics [Eq. 4].

$$\frac{C_{DNA}}{C_{DNA,0}} = \exp(-k_2 t) \tag{4}$$

where $C_{\text{DNA},0}$ represents the initial amount of pDNA encapsulated within the hydrogel [Table II]. The k_2 was further related to the degradation rate of the gel, k_1, fitted to a power law [Fig. 3b].

The effects of k_1 and k_2 on cellular gene expression were next tested with both genes encoding for GFP and genes encoding for luciferase. MVG and oxidized binary MVM gels were used, because these two formulations bracket the range of the pDNA release rates available with this group of gels. The rapidly degrading oxidized binary MVM gel resulted in the faster and higher GFP expression [Fig. 4a] and luciferase expression of cells [Fig. 4b], as compared with the unary MVG gels. The cellular GFP expression remained stable over 2 weeks, suggesting continuous uptake and expression of pDNA by cells.

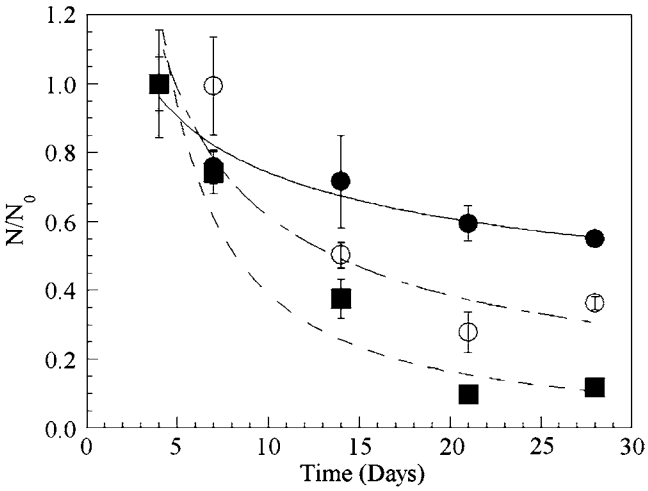

Fig. 2. Degradation rates of hydrogels were varied with the formulation; unary MVG gels (*closed circles*), oxidized binary MVG gels (*open circles*), and oxidized binary MVM gels (*closed squares*). Degradation rates of gels were evaluated by the decrease in the number of cross-links (N) of the hydrogels, normalized to the number of cross-links at day 1 (N_0), as a function of time.

Delivery of Angiogenic Genes for Revascularization

The oxidized binary MVM gel was subsequently used for the sustained delivery of pDNA encoding VEGF to the ischemic hindlimbs of mice, because this gel resulted in the

Table II. Degradation Rate (k_1) of Hydrogels and pDNA-PEI Complex Release Rate (k_2) from these Gels

Hydrogel	k_1 (day)	k_2 (day)
Unary MVG	0.02	0.005
Oxidized binary MVG	0.05	0.05
Oxidized binary MVM	0.10	0.19

The N/P ratio of pDNA-PEI complexes was kept constant at 7.

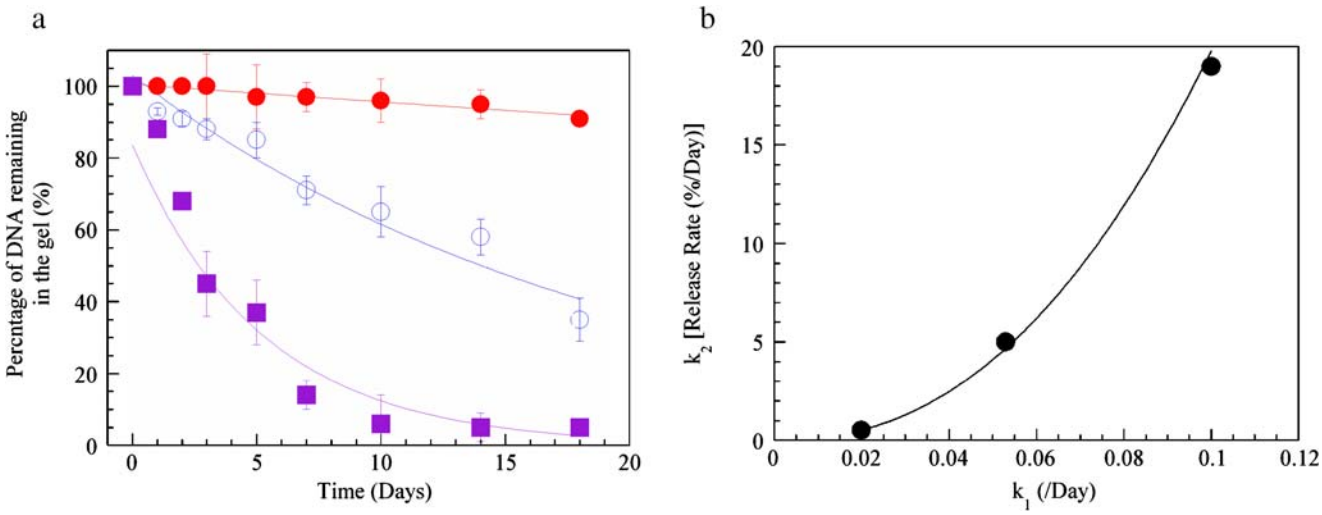

Fig. 3. The *in vitro* pDNA release was monitored from unary MVG gels (*closed circles*), oxidized binary MVG gels (*open circles*), and oxidized binary MVM gels (*closed squares*) (**a**). The pDNA release rate (k_2) was related to the degradation rate (k_1) following a power-law (**b**). The N/P ratio of pDNA-PEI complexes was kept constant at 7.

faster release of pDNA and higher gene expression level in cells over 2 weeks, as compared with other two different conditions. This time-frame of localized VEGF exposure has been recently shown to effectively drive angiogenesis (18). The sustained release of VEGF-encoding pDNA from the hydrogel significantly enhanced the recovery of blood flow in the originally ischemic right hindlimb [Fig. 5a and c], as compared with injection into the tissue with a PBS solution of pDNA-PEI complexes [Fig. 5b and c], blank PBS solution [results not shown], and hydrogel alone [results not shown].

The number of capillaries in the connective tissue and muscle adjacent to the ischemic hindlimbs were counted to examine whether the recovery of blood perfusion was related

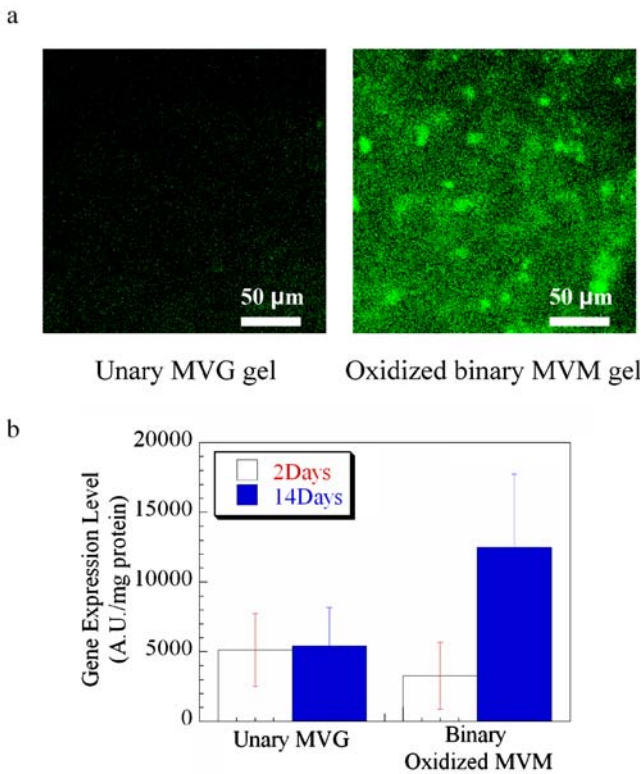

Fig. 4. The use of oxidized binary MVM hydrogels as delivery vehicles of GFP-encoding pDNA led to higher GFP expression in MC3T3-E1 cells (**a**) and higher luciferase expression in C2C12 cells (**b**) cultured within collagen gels, as compared with the use of unary MVG gels as pDNA delivery vehicles. The N/P ratio of pDNA complexes was kept constant at 7. In **b**, at 14 days, the value for oxidized binary MVM gels was statistically different ($p<0.05$), as compared to the value for unary MVG gels.

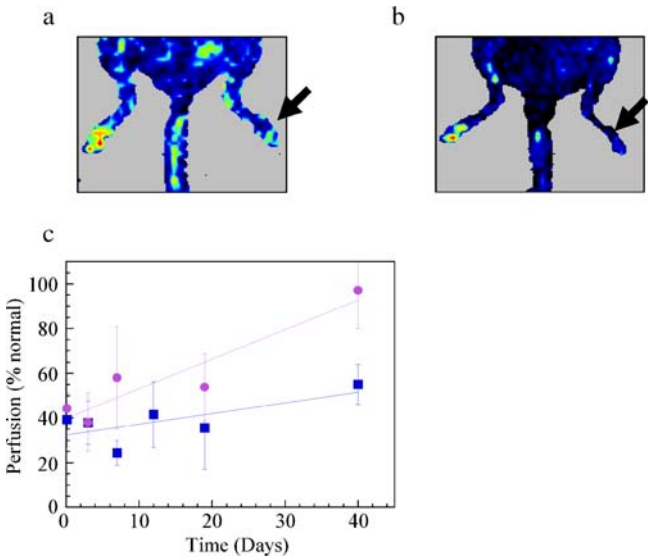

Fig. 5. The use of oxidized binary MVM hydrogels as a delivery vehicle of VEGF-encoding pDNA enhanced the blood perfusion in the ischemic hind limbs of mice (right hind limb, *arrow*) (**a**) as compared with the bolus injection of VEGF-encoding pDNAs (**b**). **a** and **b** represent laser Doppler perfusion images of a mouse hindlimb. The left limb in all mice was not ligated, and perfusion in this control limb was used to normalize perfusion levels in the experimental limb. The blood flow was quantified with this technique in five different animals when pDNA was released from the oxidized binary MVM gel [*closed circles* in **c**] or injected in solution form [curve *closed squares* in **c**]. The N/P ratio of pDNA complexes was kept constant at 7. Values represent the mean and standard deviation from five independent measurements.

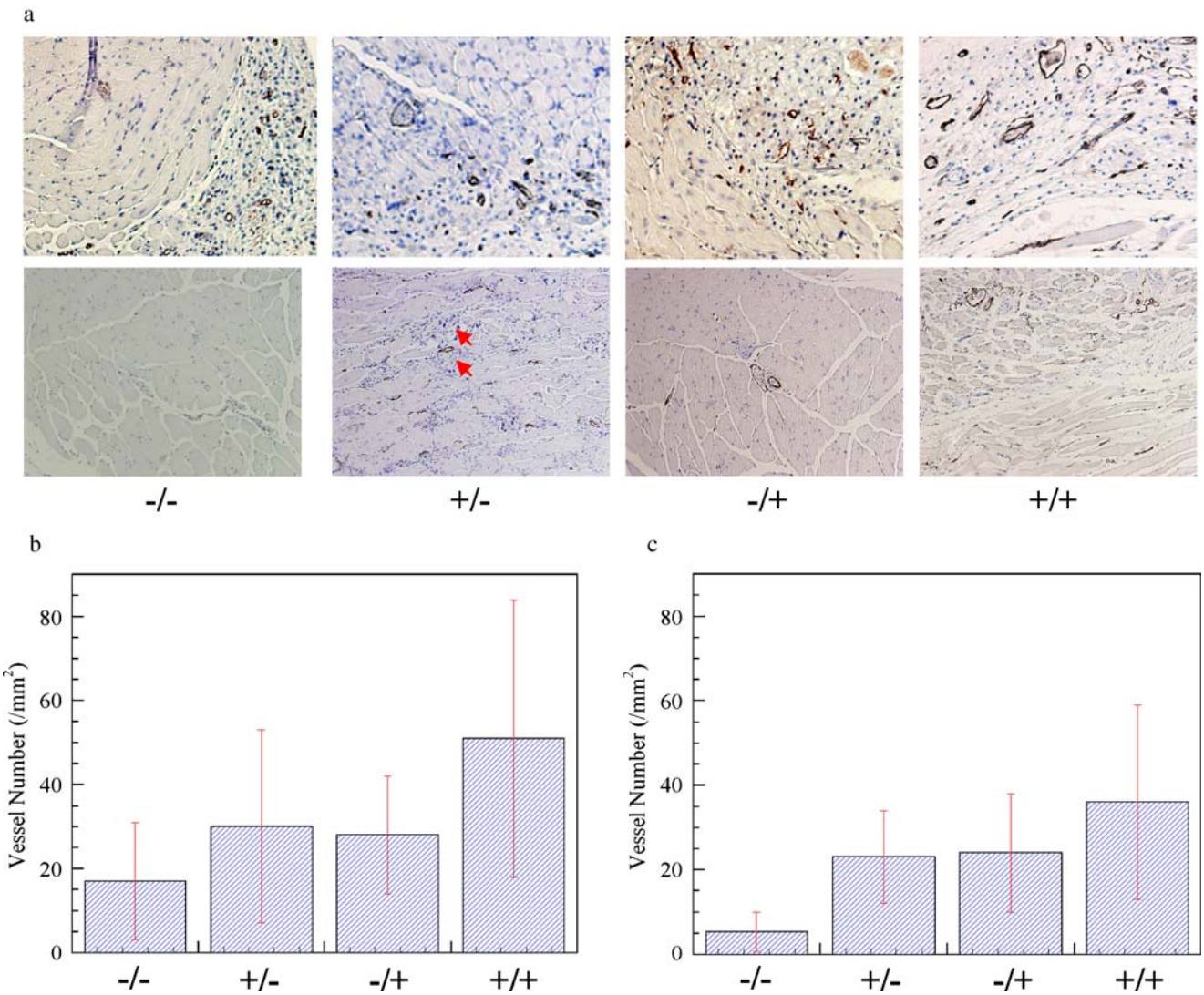

Fig. 6. The sustained delivery of VEGF-encoding pDNA using the oxidized binary MVM gels led to the largest number of blood vessels [+/+], as compared with injection of a PBS buffer [−/−], pDNA-PEI complex solution [+/−], and blank oxidized binary MVM gels [−/+]. The photomicrographs in the *upper row* of **a** are from the connective tissue, while those in the *lower row* of **a** are from the muscle tissue in the originally ischemic hind limbs. The number of blood vessels in the connective tissue (**b**), and muscle (**c**) were quantified. The N/P ratio of pDNA complexes was kept constant at 7. Values represent the mean and standard deviation from five independent experiments. In **b** and **c**, the values for release of pDNA from oxidized binary MVM gels were statistically different ($p<0.05$), as compared to values for injection of PBS solution, pDNA solution and blank oxidized binary MVM gel.

to changes in the blood vessel density (34). The blood vessel density in the connective tissue was larger than that formed in the muscle tissue, likely because the pDNA solution and pDNA-encapsulating hydrogels were injected into a pocket between the two tissues and the pDNA likely did not diffuse as effectively into the muscle tissue. The release of the pDNA from the oxidized binary MVM gel led to the largest blood vessel density within the connective tissue [upper photos in Fig. 6a and b] and muscle [lower photos in Fig. 6a and c], as illustrated with blood vessels positively stained for CD31. The average diameter of the blood vessels was also largest with the sustained release of pDNA from the hydrogel. In contrast, the bolus injection of pDNA did not significantly increases the number nor size of the blood vessels, as compared with injection of blank PBS solution or hydrogels alone. In addition, the bolus injection of the pDNA drove a significant inflammatory response in the muscle (marked with arrows in Fig. 6a), which was minimal with the sustained release of pDNA using the oxidized binary MVM gel.

DISCUSSION

The results of this study demonstrate one can enhance the angiogenic efficacy of pDNA interventions with their local and sustained delivery using biodegradable hydrogels. A hydrogel was designed to degrade via concurrent physical dissociation between cross-linking segments of polymers and hydrolytic polymer chain breakage, and the pDNA release rate from the hydrogel was significantly accelerated. The local and sustained delivery of pDNAs encoding for VEGF with these hydrogels significantly enhanced the recovery of blood perfusion in the ischemic hindlimbs of mice by promoting angiogenesis.

The degradation rate of ionically cross-linked alginate gels was accelerated by combining the concurrent separation of ionically cross-linked polymer chains using a mismatch in the size of cross-linking junctions with hydrolytic chain breakage. A previous study demonstrated that 1% oxidation of alginates selectively opened sugar rings in the blocks of mannuronic acid residues (MA block) to form hydrolytically labile acetal linkages (31). In contrast, the structure of the GA blocks responsible for the cross-linking remained intact with this treatment. Therefore, hydrolytic polymer chain breakage likely occurred on the MA blocks in the oxidized binary MVG and oxidized binary MVM gels [Fig. 1e]. In addition, the cross-linking junction formed with GA blocks of different molecular weights was found to be more labile to ion-exchange than the cross-linking junction formed with GA blocks of the same molecular weight [Fig. 1f]. Therefore, the cross-linking junctions in the oxidized binary MVM hydrogels dissociated faster than the cross-linking junction in the unary MVG gels and oxidized binary MVG gels (30).

Rapid degradation of these gels was advantageous in controlling pDNA release and exogenous gene expression without denaturation of the encapsulated pDNA. The minimal release of pDNAs from the unary MVG gel indicated that the pDNAs could not diffuse through nanopores of these hydrogels, because the pore structure remained stable, or, the electrostatic attraction between pDNA-PEI complexes and alginate molecules sequestered the pDNAs within the hydrogel. In contrast, the accelerated dissolution of the oxidized binary MVG and MVM gels increased the pDNA release, as confirmed with the power-law relationship between the hydrogel degradation rate and the pDNA release rate. Subsequently, the increase in pDNAs released from oxidized binary MVM gels led to a higher gene expression level in cells. Subsequently, pDNAs rapidly released from oxidized binary MVM gels led to the higher gene expression level of cells. It is possible that the cells may exhibit longer-term gene expression in a 3D environment, when using these degrading gels, as has been demonstrated in a previous report (35).

Revascularization in ischemic hindlimbs was enhanced with use of the oxidized binary MVM gel as a delivery vehicle of VEGF-encoding pDNA. The pDNA delivery using the gel likely increased the local concentration of pDNA in the ischemic region, allowing host cells to take up larger numbers of pDNA molecules. In addition, the sustained release of the pDNA may have led host cells to repeatedly take up and express the pDNAs (36). In consequence, the activities of vascular cells in forming capillaries were likely stimulated due to the local increase and duration of VEGF signaling. Interestingly, the bolus injection of pDNA-PEI complexes stimulated the recruitment of inflammatory cells, perhaps due to the high local concentration of PEI, which has been demonstrated to lead to inflammation. In contrast, sustained delivery of the same total quantity of pDNA-PEI did not lead to this inflammation, likely due to lower local concentration of PEI at any time.

Overall, this study demonstrated a new strategy to control the pDNA release rate over a broad range by combining two different degradation processes of biomaterials. We envisage that this strategy may be highly useful to controlling the delivery of a wide array of nucleotide therapies (e.g., RNA, viral genes) (37) and proteins (e.g., growth factors and antibodies) (18).

ACKNOWLEDGEMENT

The authors thank the NIH (RO1 DE013033 and RO1 HL069957) for the financial support of this research. The authors also thank Mr. Francis Rauh of FMC Corporation for supplying the alginate samples.

REFERENCES

1. D. W. Losordo and S. Dimmeler. Therapeutic angiogenesis and vasculogenesis for ischemic disease—Part II: Cell-based therapies. *Circulation* **109**:2692–2697 (2004).
2. D. W. Losordo and S. Dimmeler. Therapeutic angiogenesis and vasculogenesis for ischemic disease—Part I: Angiogenic cytokines. *Circulation* **109**:2487–2491 (2004).
3. J. M. Isner. Myocardial gene therapy. *Nature* **415**:234–239 (2002).
4. A. A. Kocher, M. D. Schuster, M. J. Szabolcs, S. Takuma, D. Burkhoff, J. Wang, S. Homma, N. M. Edwards, and S. Itescu. Neovascularization of ischemic myocardium by human bone-marrow-derived angioblasts prevents cardiomyocyte apoptosis, reduces remodeling and improves cardiac function. *Nat. Med.* **7**:430–436 (2001).
5. J. M. Isner and D. W. Losordo. Therapeutic angiogenesis for heart failure. *Nat. Med.* **5**:491–492 (1999).
6. T. P. Richardson, M. C. Peters, A. B. Ennett, and D. J. Mooney. Polymeric system for dual growth factor delivery. *Nat. Biotechnol.* **19**:1029–1034 (2001).
7. F. J. Giordano, P. P. Ping, M. D. McKirnan, S. Nozaki, A. N. DeMaria, W. H. Dillmann, O. MathieuCostello, and H. K. Hammond. Intracoronary gene transfer of fibroblast growth factor-5 increases blood flow and contractile function in an ischemic region of the heart. *Nat. Med.* **2**:534–539 (1996).
8. Y. Tsurumi, S. Takeshita, D. F. Chen, M. Kearney, S. T. Rossow, J. Passeri, J. R. Horowitz, J. F. Symes, and J. M. Isner. Direct intramuscular gene transfer of naked DNA encoding vascular endothelial growth factor augments collateral development and tissue perfusion. *Circulation* **94**:3281–3290 (1996).
9. S. Takeshita, Y. Tsurumi, T. Couffinahl, T. Asahara, C. Bauters, J. Symes, N. Ferrara, and J. M. Isner. Gene transfer of naked DNA encoding for three isoforms of vascular endothelial growth factor stimulates collateral development *in vivo*. *Lab. Invest.* **75**:487–501 (1996).
10. X. J. Hao, A. Mansson-Broberg, P. Blomberg, G. Dellgren, A. J. Siddiqui, K. H. Grinnemo, E. Wardell, and C. Sylven. Angiogenic and cardiac functional effects of dual gene transfer of VEGF-A(165) and PDGF-BB after myocardial infarction. *Biochem. Biophys. Res. Commun.* **322**:292–296 (2004).
11. A. J. Comerota, R. C. Throm, K. A. Miller, T. Henry, N. Chronos, J. Laird, R. Sequeira, C. K. Kent, M. Bacchetta, C. Goldman, J. P. Salenius, F. A. Schmieder, and R. Pilsudski. Naked plasmid DNA encoding fibroblast growth factor type I for the treatment of end-stage unreconstructible lower extremity ischemia: Preliminary results of a phase I trial. *J. Vasc. Surg.* **35**:930–936 (2002).
12. C. Madeira, L. M. S. Loura, M. R. Aires-Barros, A. Fedorov, and M. Prieto. Characterization of DNA/lipid complexes by fluorescence resonance energy transfer. *Biophys. J.* **85**:3106–3119 (2003).
13. M. D. Brown, A. G. Schatzlein, and I. F. Uchegbu. Gene delivery with synthetic (non viral) carriers. *Int. J. Pharm.* **229**:1–21 (2001).
14. C. L. Densmore, F. M. Orson, B. Xu, B. M. Kinsey, J. C. Waldrep, P. Hua, B. Bhogal, and V. Knight. Aerosol delivery of robust polyethyleneimine-DNA complexes for gene therapy and genetic immunization. *Molec. Ther.* **1**:180–188 (2000).
15. L. J. Branden, A. J. Mohamed, and C. I. E. Smith. A peptide nucleic acid-nuclear localization signal fusion that mediates nuclear transport of DNA. *Nat. Biotechnol.* **17**:784–787 (1999).

16. R. C. Adami, W. T. Collard, S. A. Gupta, K. Y. Kwok, J. Bonadio, and K. G. Rice. Stability of peptide condensed plasmid DNA formulations. *J. Pharm. Sci.* **87**:678–683 (1998).
17. P. L. Felgner, T. R. Gadek, M. Holm, R. Roman, H. W. Chan, M. Wenz, J. P. Northrop, G. M. Ringold, and M. Danielsen. Lipofection—A highly efficient, lipid-mediated DNA-transfection procedure. *Proc. Natl. Acad. Sci. U. S. A.* **84**:7413–7417 (1987).
18. E. A. Silva and D. J. Mooney. Spatiotemporal control of vascular endothelial growth factor delivery from injectable hydrogels enhances angiogenesis. *J. Thrombos. Haemost.* **5**:590–598 (2007).
19. D. H. Walter, M. Cejna, L. Diaz-Sandoval, S. Willis, L. Kirkwood, P. W. Stratford, A. B. Tietz, R. Kirchmair, M. Silver, C. Curry, A. Wecker, Y. S. Yoon, R. Heidenreich, A. Hanley, M. Kearney, F. O. Tio, P. Kuenzler, J. M. Isner, and D. W. Losordo. Local gene transfer of phVEGF-2 plasmid by gene-eluting stents—An alternative strategy for inhibition of restenosis. *Circulation* **110**:36–45 (2004).
20. Y. X. Lu, J. Shansky, M. Del Tatto, P. Ferland, X. Y. Wang, and H. Vandenburgh. Recombinant vascular endothelial growth factor secreted from tissue-engineered bioartificial muscles promotes localized angiogenesis. *Circulation* **104**:594–599 (2001).
21. J. Bonadio, E. Smiley, P. Patil, and S. Goldstein. Localized, direct plasmid gene delivery *in vivo*: prolonged therapy results in reproducible tissue regeneration. *Nat. Med.* **5**:753–759 (1999).
22. L. De Laporte and L. D. Shea. Matrices and scaffolds for DNA delivery in tissue engineering. *Adv. Drug Deliv. Rev.* **59**:292–307 (2007).
23. J. H. Jang, C. B. Rives, and L. D. Shea. Plasmid delivery *in vivo* from porous tissue-engineering scaffolds: Transgene expression and cellular tansfection. *Molec. Ther.* **12**:475–483 (2005).
24. S. Jilek, H. Zurkaulen, J. Pavlovic, H. P. Merkle, and E. Walter. Transfection of a mouse dendritic cell line by plasmid DNA-loaded PLGA microparticles *in vitro*. *Eur. J. Pharm. Biopharm.* **58**:491–499 (2004).
25. J. H. Jeong and T. G. Park. Novel polymer-DNA hybrid polymeric micelles composed of hydrophobic poly(D,L-lactic-co-glycolic acid) and hydrophilic oligonucleotides. *Bioconjug. Chem.* **12**:917–923 (2001).
26. Y. Fukunaka, K. Iwanaga, K. Morimoto, M. Kakemi, and Y. Tabata. Controlled release of plasmid DNA from cationized gelatin hydrogels based on hydrogel degradation. *J. Control. Release* **80**:333–343 (2002).
27. Z. H. Li, W. Ning, J. M. Wang, A. Choi, P. Y. Lee, P. Tyagi, and L. Huang. Controlled gene delivery system based on thermosensitive biodegradable hydrogel. *Pharm. Res.* **20**:884–888 (2003).
28. F. K. Kasper, S. K. Seidlits, A. Tang, R. S. Crowther, D. H. Carney, M. A. Barry, and A. G. Mikos. *In vitro* release of plasmid DNA from oligo(poly(ethylene glycol) fumarate) hydrogels. *J. Control. Release* **104**:521–539 (2005).
29. J. A. Wieland, T. L. Houchin-Ray, and L. D. Shea. Non-viral vector delivery from PEG-hyaluronic acid hydrogels. *J. Control. Release* **120**:233–241 (2007).
30. H. J. Kong, E. Alsberg, D. Kaigler, K. Y. Lee, and D. J. Mooney. Controlling degradation of hydrogels via the size of cross-linked junctions. *Adv. Mater.* **16**:1917–1921 (2004).
31. H. J. Kong, D. Kaigler, K. Kim, and D. J. Mooney. Controlling rigidity and degradation of alginate hydrogels via molecular weight distribution. *Biomacromolecules* **5**:1720–1727 (2004).
32. K. S. Anseth, C. N. Bowman, and L. BrannonPeppas. Mechanical properties of hydrogels and their experimental determination. *Biomaterials* **17**:1647–1657 (1996).
33. H. J. Kong, S. Hsiong, and D. J. Mooney. Nanoscale cell adhesion ligand presentation regulates nonviral gene delivery and expression. *Nano Lett.* **7**:161–166 (2007).
34. T. Couffinhal, M. Silver, L. P. Zheng, M. Kearney, B. Witzenbichler, and J. M. Isner. Mouse model of angiogenesis. *Am. J. Pathol.* **152**:1667–1679 (1998).
35. Y. B. Xie, S. T. Yang, and D. A. Kniss. Three-dimensional cell-scaffold constructs promote efficient gene transfection: Implications for cell-based gene therapy. *Tissue Eng.* **7**:585–598 (2001).
36. N. J. Meilander-Lin, P. J. Cheung, D. L. Wilson, and R. V. Bellamkonda. Sustained *in vivo* gene delivery from agarose hydrogel prolongs nonviral gene expression in skin. *Tissue Eng.* **11**:546–555 (2005).
37. S. Jain, W. T. Yap, and D. J. Irvine. Synthesis of protein-loaded hydrogel particles in an aqueous two-phase system for coincident antigen and CpG oligonucleotide delivery to antigen-presenting cells. *Biomacromolecules* **6**:2590–2600 (2005).